Step Convergence Analysis of Nonlinear Feedback Hysteresis Models*

JinHyoung Oh and Dennis S. Bernstein[†]

Abstract— In this paper we consider nonlinear feedback hysteresis models. Since hysteresis is defined as a nontrivial input-output map under quasi-DC inputs, the relationship between step convergence and the hysteresis map of the model is investigated. The class of models that exhibit hysteresis is determined and the shape of the hysteresis map is characterized. We focus on the deadzone nonlinearity, which has implications for backlash modeling. Numerical examples are presented to verify the analysis.

I. INTRODUCTION

Hysteresis arises in diverse applications, including structural mechanics, aerodynamics, and electromagnetics. The word "hysteresis" connotes lag, although this nomenclature is misleading since delay per se is not the mechanism that gives rise to hysteresis. In this paper we show that multistability is the essential mechanism for hysteresis. Similar observations have been made in [1], [2], [3], [4].

Hysteretic systems are generally described as having memory. A more precise system-theoretic definition of hysteresis is the persistence of a nondegenerate input-output closed curve as the frequency of excitation tends toward DC. Such systems are inherently nonlinear since a linear system can have a quasi-DC phase shift corresponding to only a multiple of $\pi/2$. A hysteretic system whose input-output behavior is independent of frequency is called *rate independent*; when the periodic steady-state input-output behavior depends on the input frequency, the hysteretic system is *rate dependent*.

Various nonlinearities can give rise to hysteresis, as reflected by the diverse models that have been studied. The classical Preisach model [5] is given in terms of an integral whose kernel determines the shape of the hysteresis map; such models are generally rate independent. Alternatively, the finite-dimensional Duhem model [6], [7] is modeled by an ordinary differential equation whose vector field depends on the derivative of the input. The Duhem model can be either rate independent or rate dependent. Yet another model of hysteresis is the bifurcation model, in which a nonlinear feedback map gives rise to multiple asymptotically stable equilibria, the number of which varies as a function of the input [8, p. 17].

In mechanical engineering applications, perhaps the most familiar example of hysteresis is the backlash model, which represents free play in mechanical couplings. In practice, backlash often represents one of the main impediments to achievable performance, and efforts to model backlash and reduce its impact remain an active area of research [9], [10], [11], [12]. In its simplest form, backlash can be viewed as a feedback loop involving linear dynamics and a deadzone function. For example, the system in Figure 1 depicts a mechanical system with a free play interconnection, while the corresponding block diagram shown in Figure 2 consists of a feedback interconnection with a deadzone nonlinearity. As shown in Figure 3 and noted in [13], this hysteretic system is rate dependent.

A slightly more complex example of the backlash model is given by the flexible rotating shafts in Figure 4 interconnected by a freeplay. In this case, the block diagrams in Figure 2 must be extended to the linear fractional transformation given in Figure 5.

A common feature of all of the above hysteresis models is multistability, that is, the existence of multiple attracting equilibria. The attracting equilibria may be isolated or they may constitute a continuum. In particular, the Duhem model has the property that, for every constant input, every state of the system is an equilibrium. In contrast, the bifurcation model has a finite number of isolated equilibria, while the backlash model has a continuum of equilibria that constitute a strip region in the input-output plane. An equilibrium that is not isolated cannot be asymptotically stable, although it can be semistable. The semistable equilibria, which constitute a subset of the Lyapunov-stable equilibria, are those equilibria for which a trajectory beginning in a neighborhood converges to a Lyapunov stable equilibrium; for details, see [14], [15]

In either case, that is, isolated or nonisolated, what is important from the point of view of hysteresis is the fact that the trajectory converges for constant inputs. Step convergence refers to the convergence of trajectories to
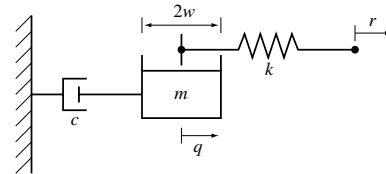

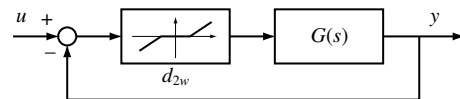Fig. 1.   Mass-dashpot-spring system with a deadzone.

Fig. 2.   Block diagram representation of the deadzone-based hysteresis model. For the mass-dashpot-spring system with a deadzone shown in Figure 1, $G(s) = k/(ms^2 + cs)$ with $u = r$ and $y = q$.
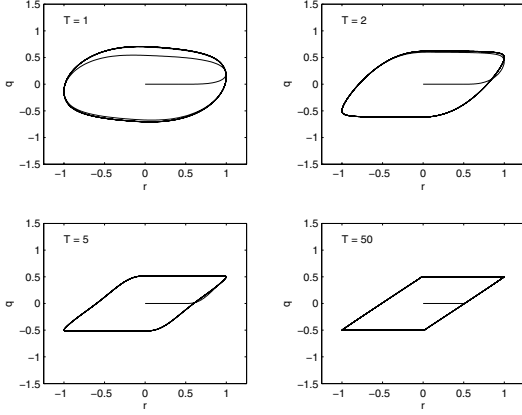
Fig. 3. Input-output map for the mass-dashpot-spring system with a deadzone where $w = 0.5$, $m = 0.1$, $k = 10$, $c = 1$, and $r(t) = \sin \frac{2\pi}{T} t$.
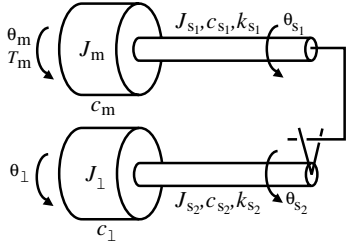

Fig. 4. Mechanical system with two flexible rotating shafts interconnected by a freeplay.

equilibria for all constant inputs. The relevance of step convergence to the existence of hysteresis lies in the fact that, in the quasi-DC limit, the system response depends on the convergence of the state for all constant, that is, step, inputs.

The goal of the present paper is to formulate and analyze nonlinear feedback models that give rise to hysteresis. In particular, we consider an extension of the system shown in Figure 2, where now the transfer function $G(s)$ need not be of the special form $G(s) = k/(ms^2 + cs)$. Then we generalize the model to the system shown in Figure 5. Our goal is to determine a class of transfer functions for which the closed-loop system with a deadzone nonlinearity is hysteretic, and to characterize the shape of the hysteresis map.
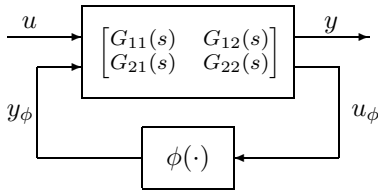

Fig. 5. A linear fractional transformation involving a two-input/two-output linear system and a nonlinearity. The mechanical system with a freeplay in Figure 4 can be modeled with a deadzone nonlinearity ϕ. The variables u, y, u_ϕ, y_ϕ denote $T_m, \theta_l, \theta_{s_2}, \theta_{s_1}$ in Figure 4, respectively.

The contents of the paper are as follows. In Section 2 we introduce the deadzone-based hysteresis model and define the limiting equilibria set and the hysteresis map. In Section 3, we investigate the step convergence of the deadzone-based backlash hysteresis model. Then we characterize the shape of the hysteresis map for different classes of the model in Section 4. Finally, we consider the nonlinear feedback model as a generalization, followed by Conclusions.

II. DEADZONE-BASED HYSTERESIS MODEL

Consider the *deadzone-based hysteresis model*

$$\dot{x}(t) = Ax(t) - Bd_{2w}\big(y(t) - u(t)\big), \tag{1}$$

$$y(t) = Cx(t), \qquad x(0) = x_0, \quad t \geq 0, \tag{2}$$

where $A \in \mathbb{R}^{n \times n}$, $B \in \mathbb{R}^n$, $C \in \mathbb{R}^{1 \times n}$, $u : [0, \infty) \to \mathbb{R}$ is continuous and piecewise $\mathbf{C}^1$, and $d_{2w} : \mathbb{R} \to \mathbb{R}$ is a deadzone function with a width $2w$ given by

$$d_{2w}(v) \triangleq \begin{cases} v - w, & v > w, \\ 0, & |v| \leq w, \\ v + w, & v < -w. \end{cases} \tag{3}$$

Since the deadzone function is globally Lipschitz, the solution to (1) exists and is unique on all finite intervals. We also assume that (A, B, C) is minimal. Note that (1), (2) can be represented as the block diagram shown in Figure 2 with $G(s) \triangleq C(sI - A)^{-1}B$.

Since (A, B, C) is minimal, let A, B, and C be given in the controllable canonical form

$$A = \begin{bmatrix} 0 & 1 & \cdots & 0 \\ \vdots & \vdots & \ddots & \vdots \\ 0 & 0 & \cdots & 1 \\ -a_0 & -a_1 & \cdots & -a_{n-1} \end{bmatrix}, \quad B = \begin{bmatrix} 0 \\ \vdots \\ 0 \\ 1 \end{bmatrix}, \tag{4}$$

$$C = \begin{bmatrix} c_0 & c_1 & \cdots c_{n-1} \end{bmatrix}.$$

Suppose $u(t) = \bar{u}$ is constant. Then the equilibrium $\bar{x}$ of (1) is given by

$$\bar{x} = \begin{bmatrix} \bar{x}_1 & 0 & \cdots & 0 \end{bmatrix}^\mathrm{T}, \tag{5}$$

where $\bar{x}_1$ satisfies

$$a_0 \bar{x}_1 + d_{2w}\big(c_0 \bar{x}_1 - \bar{u}\big) = 0. \tag{6}$$

Note that $\bar{x}$ is determined only by a_0 and c_0. The following definition will be needed.

Definition 2.1: The *limiting equilibria set* $\mathcal{E}$ of (1), (2) is the set of points $(\bar{u}, C\bar{x}) \in \mathbb{R}^2$, where $\bar{u}$ and $\bar{x}$ satisfy (5) and (6).

The limiting equilibria set $\mathcal{E}$ is a possibly multivalued map between $\bar{u} \in \mathbb{R}$ and the corresponding equilibria of (1) determined by (2). Note that $\mathcal{E}$ is nonempty since, for all $\bar{u} \in [-w, w]$, $\bar{x}_1 = 0$ satisfies (6) and thus $\{(\bar{u}, 0) : \bar{u} \in [-w, w]\} \subseteq \mathcal{E}$.

We can characterize the limiting equilibria set $\mathcal{E}$ of (1), (2) by analyzing the solution of (6) in the following cases.

698

Case 1: Let $a_0 \neq 0$ and $a_0 + c_0 = 0$. Then (6) has the unique solution $\bar{x}_1 = 0$ for $|u| < w$, or the continuum of solutions $\bar{x}_1 = \{x \in \mathbb{R} : x \geq 0\}$ for $u = w$ and $\bar{x}_1 = \{x \in \mathbb{R} : x \leq 0\}$ for $u = -w$. Hence $\mathcal{E}$ is given by

$$
\begin{aligned}
\mathcal{E} = &\{(w, y) \in \mathbb{R}^2 : y \geq 0\} \\
&\cup \{(u, y) \in \mathbb{R}^2 : |u| \leq w, y = 0\} \qquad (7) \\
&\cup \{(-w, y) \in \mathbb{R}^2 : y \leq 0\}.
\end{aligned}
$$

Case 2: Let $a_0 = 0$. Then, for all $u \in \mathbb{R}$, (6) has the continuum of solutions $\bar{x}_1 = \{x \in \mathbb{R} : \frac{u-w}{c_0} \leq x \leq \frac{u+w}{c_0}\}$ for $c_0 > 0$ and $\bar{x}_1 = \{x \in \mathbb{R} : \frac{u+w}{c_0} \leq x \leq \frac{u-w}{c_0}\}$ for $c_0 < 0$. Hence $\mathcal{E}$ is given by

$$
\mathcal{E} = \left\{(u, y) \in \mathbb{R}^2 : u - w \leq y \leq u + w, \ u \in \mathbb{R}\right\}. \quad (8)
$$

Case 3: Let $a_0 \neq 0$ and $a_0 c_0 \geq 0$, or $a_0 \neq 0$ and $c_0(a_0 + c_0) < 0$. Then (6) has the unique solution $\bar{x}_1 = \frac{1}{a_0 + c_0} d_{2w}(u)$ for all $u \in \mathbb{R}$. Hence $\mathcal{E}$ is given by

$$
\mathcal{E} = \left\{ \left(u, \frac{c_0}{a_0 + c_0} d_{2w}(u)\right) \in \mathbb{R}^2 : u \in \mathbb{R} \right\}. \quad (9)
$$

Case 4: Let $a_0 \neq 0$ and $c_0(a_0 + c_0) > 0$. Then (6) has the unique solution $\bar{x}_1 = \frac{u+w}{a_0 + c_0}$ for $u > w$ and $\bar{x}_1 = \frac{u-w}{a_0 + c_0}$ for $u < -w$, or non-unique solutions $\bar{x}_1 = \{\frac{u-w}{a_0 + c_0}, 0, \frac{u+w}{a_0 + c_0}\}$ for $|u| < w$. Hence $\mathcal{E}$ is given by

$$
\begin{aligned}
\mathcal{E} = &\left\{ \left(u, \frac{c_0(u + w)}{a_0 + c_0}\right) \in \mathbb{R}^2 : u > -w \right\} \\
&\cup \left\{(u, 0) \in \mathbb{R}^2 : |u| < w\right\} \qquad (10) \\
&\cup \left\{ \left(u, \frac{c_0(u - w)}{a_0 + c_0}\right) \in \mathbb{R}^2 : u < w \right\}.
\end{aligned}
$$

Figure 6 shows that the limiting equilibria set $\mathcal{E}$ for each case given by (7)–(10). The following definitions will be useful.
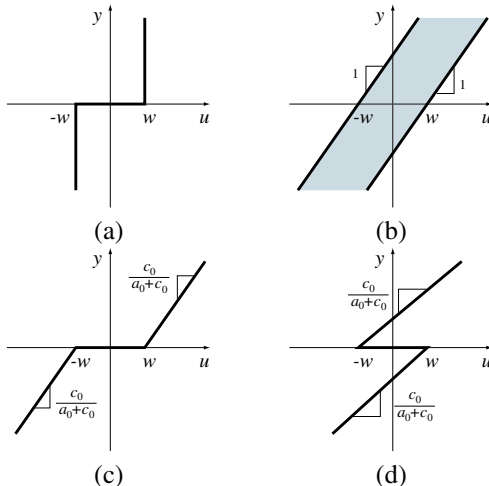

Fig. 6. The limiting equilibria set $\mathcal{E}$ of (a) case 1 given by (7), (b) case 2 given by (8), (c) case 3 given by (9), and (d) case 4 given by (10).

Definition 2.2: The nonempty set $\mathcal{H} \subset \mathbb{R}^2$ is a *closed curve* if there exists a continuous, piecewise C^1, and periodic map $\gamma : [0, \infty) \to \mathbb{R}^2$ such that $\gamma([0, \infty)) = \mathcal{H}$.

Definition 2.2 implies that every closed curve is a compact and connected subset of $\mathbb{R}^2$. For closed curves $\mathcal{H}_1, \mathcal{H}_2$, define the Hausdorff metric [16, p. 104]

$$
\begin{aligned}
&d(\mathcal{H}_1, \mathcal{H}_2) \\
&\triangleq \max \left\{ \sup_{\eta_1 \in \mathcal{H}_1} \left(\inf_{\eta_2 \in \mathcal{H}_2} \|\eta_1 - \eta_2\| \right), \sup_{\eta_2 \in \mathcal{H}_2} \left(\inf_{\eta_1 \in \mathcal{H}_1} \|\eta_1 - \eta_2\| \right) \right\},
\end{aligned}
$$

where $\| \cdot \|$ is a norm on $\mathbb{R}^2$. Since $\mathbb{R}^2$ with the metric $d(x, y) \triangleq \|x - y\|$ is complete, the set of closed curves with $d(\cdot, \cdot)$ is a complete metric space.

Definition 2.3: Let $u : [0, \infty) \to [u_{\min}, u_{\max}]$ be continuous, piecewise C^1, periodic with period α, and have exactly one local maximum $u_{\max}$ in $[0, \alpha)$ and exactly one local minimum $u_{\min}$ in $[0, \alpha)$. For all $T > 0$, define $u_T(t) \triangleq u(\alpha t / T)$, assume that there exists $x_T : [0, \infty) \to \mathbb{R}^n$ that is periodic with period T and satisfies (1) with $u = u_T$, and let $y_T : [0, \infty) \to \mathbb{R}$ be given by (2) with $x = x_T$ and $u = u_T$. For all $T > 0$, the *periodic input-output map* $\mathcal{H}_T(u_T, y_T)$ is the closed curve $\mathcal{H}_T(u_T, y_T) \triangleq \{(u_T(t), y_T(t)) : t \in [0, \infty)\}$, and the *limiting periodic input-output map* $\mathcal{H}_\infty(u)$ is the closed curve $\mathcal{H}_\infty(u) \triangleq \lim_{T \to \infty} \mathcal{H}_T(u_T, y_T)$ if the limit exists and is independent of y_T. If there exist $(u, y_1), (u, y_2) \in \mathcal{H}_\infty(u)$ such that $y_1 \neq y_2$, then $\mathcal{H}_\infty(u)$ is a *hysteresis map*, and the deadzone-based hysteresis model is *hysteretic*.

Example 2.1: Reconsider the mass/dashpot/spring with gap in Figure 1 modeled by

$$
m\ddot{x}(t) + c\dot{x}(t) + k d_{2w}\big(x(t) - u(t)\big) = 0, \qquad (11)
$$

with $x(0) = x_0$, $t \geq 0$. The model (11) is equivalent to (1), (2) with

$$
A = \begin{bmatrix} 0 & 1 \\ 0 & -\frac{c}{m} \end{bmatrix}, \ B = \begin{bmatrix} 0 \\ 1 \end{bmatrix}, \ C = \begin{bmatrix} \frac{k}{m} & 0 \end{bmatrix}.
$$

Since $a_0 = 0$, (11) satisfies case 2 and the limiting equilibria set $\mathcal{E}$ of (11) is given by $\mathcal{E} = \{(u, y) \in \mathbb{R}^2 : u - w \leq y \leq u + w, \ u \in \mathbb{R}\}$.

Now, setting $A = 0$, $B = \frac{k}{m}$, and $C = 1$ yields the single integrator with deadzone hysteresis model [13]

$$
m\dot{x}(t) + k d_{2w}\big(x(t) - u(t)\big) = 0. \qquad (12)
$$

Since $A = a_0 = 0$, (12) also satisfies case 2 and thus $\mathcal{E} = \{(u, y) \in \mathbb{R}^2 : u - w \leq y \leq u + w, \ u \in \mathbb{R}\}$. Note that $\mathcal{E}$ of (11) and $\mathcal{E}$ of (12) are identical, since a_0 is the same for both models.

III. Step Convergence and the Deadzone-Based Hysteresis Model

In this section we investigate the relationship between step convergence and the deadzone-based hysteresis model

(1), (2). The following definition modified from [15] is needed.

Definition 3.1: Consider (1) with constant $u(t) = \bar{u}$. The system (1) is *step convergent* if $\lim_{t \to \infty} x(t)$ exists for all $x_0 \in \mathbb{R}^n$ and for all $\bar{u} \in \mathbb{R}$.

Suppose (1) is step convergent. Then it follows from [15] that $\lim_{t \to \infty} x(t)$ exists for every constant $u(t) = \bar{u}$ and is an equilibrium of (1). Now, let $u(t) \in [u_{\min}, u_{\max}]$ be periodic with period α. Let $u_T(t) = u(\alpha t/T)$ and suppose the periodic input-output map $\mathcal{H}_T(u_T, y_T)$ exists for all $T > 0$. Furthermore, assume the limiting periodic input-output map $\mathcal{H}_\infty(u)$ exists.

Definitions 2.3 and 3.1 suggest that there exists a close relationship between $\mathcal{H}_\infty(u)$ and the limiting equilibria set $\mathcal{E}$ of (1), (2). The set $\mathcal{H}_\infty(u)$ represents the response of the system in the limit of DC operation. Therefore, each element of $\mathcal{H}_\infty(u)$ can be viewed as the limit of a sequence of points of $\mathcal{H}_T(u_T, y_T)$ as $T \to \infty$, that is, for increasingly slower inputs. Consequently, the limiting point $(\bar{u}, \bar{y}) \in \mathcal{H}_\infty(u)$ arises from an equilibrium under the constant input $u(t) = \bar{u}$. This observation indicates that the step convergence of (1), (2) is a necessary condition for the existence of $\mathcal{H}_\infty(u)$.

However, not every limiting point in $\mathcal{H}_\infty(u)$ is in $\mathcal{E}$. If (1), (2) has a bifurcation, that is, a change in the qualitative structure of the equilibria as u changes, then the solution of (1), (2) can alternate between the subsets of $\mathcal{E}$. In this particular case, the limiting periodic input-output map $\mathcal{H}_\infty(u)$ contains vertical components that connect subsets as illustrated in Example 4.2 below. With the exception of the vertical transition trajectories between subsets of $\mathcal{E}$, this observation suggests that $\mathcal{H}_\infty(u) \subseteq \mathcal{E}$.

The relationship between $\mathcal{H}_\infty(u)$ and $\mathcal{E}$ elucidates the mechanism of hysteresis in the nonlinear feedback hysteresis model. Since Definition 2.3 requires that the hysteretic limiting periodic input-output map have (at least) two distinct points (u, y_1) and (u, y_2), a necessary condition for (1), (2) to be hysteretic is that $\mathcal{E}$ be a multivalued map.

Example 3.1: Consider (1), (2) with

$$A = \begin{bmatrix} 0 & 1 \\ 0 & 2 \end{bmatrix}, \ B = \begin{bmatrix} 0 \\ 1 \end{bmatrix}, \ C = \begin{bmatrix} 2 & 3 \end{bmatrix},$$

and $w = 0.5$. Figure 7 shows the step response with $u(t) = 0.5$ and $x_0 = \begin{bmatrix} 1 & 2 \end{bmatrix}^T$. Since $x(t)$ does not converge as $t \to \infty$, this system is not step convergent. Figure 8 shows the input-output map with $u(t) = \sin \omega t$. Since the model is not step convergent, $\mathcal{H}_\infty(u)$ does not exist.

Example 3.2: Reconsider the mass/dashpot/spring with gap modeled by (11) with $u_T(t) = \sin \frac{2\pi}{T} t$. Figure 3 shows that $\mathcal{H}_T(u_T, y_T)$ converges to a hysteretic limiting input-output map, and thus (11) is hysteretic. Note that $\mathcal{E}$ consists of points arising from a continuum of input-dependent equilibria. Suppose u_T is sufficiently slow and the solution
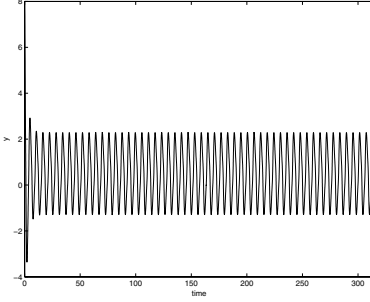

Fig. 7. Step response of Example 3.1 with $x_0 = \begin{bmatrix} 1 & 2 \end{bmatrix}^T$ and $u(t) = 0.5$. Note that $y(t)$ does not converge and the model is not step convergent.
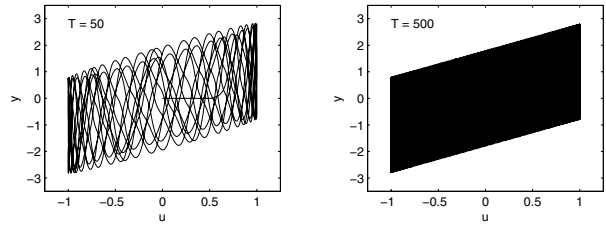

Fig. 8. Input-output maps of Example 3.1 with $u(t) = \sin \frac{2\pi}{T} t$. Note that the model is not step convergent, and thus $\mathcal{H}_\infty(u)$ does not exist.

of (11) converges to an equilibrium in the continuum of equilibria, and thus (u_T, y_T) is in the interior of $\mathcal{E}$. When u_T changes, the state remains in the continuum of equilibria and thus y_T is constant. Therefore (u_T, y_T) horizontally traverses the interior of $\mathcal{E}$ until it reaches the boundary of $\mathcal{E}$. Now when (u_T, y_T) leaves the boundary of $\mathcal{E}$, the solution returns to the boundary of the set of continua, and (u_T, y_T) follows the boundary of $\mathcal{E}$ as u_T changes. Consequently, the limiting input-output map $\mathcal{H}_\infty(u)$ of (11) consists of two horizontal components and parts of the boundary of $\mathcal{E}$ as shown in Figure 9.

IV. HYSTERESIS MAP OF THE STEP-CONVERGENT DEADZONE-BASED HYSTERESIS MODEL

In this section we consider the step-convergent deadzone-based hysteresis model (1), (2) and investigate the resulting hysteresis maps. Specifically, let (1), (2) be step convergent.
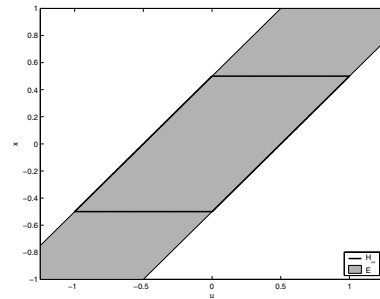

Fig. 9. $\mathcal{E}$ and $\mathcal{H}_\infty(u)$ of the mass/dashpot/spring with deadzone model in Example 3.2. $\mathcal{H}_\infty(u)$ consists of two horizontal components and parts of the boundary of $\mathcal{E}$
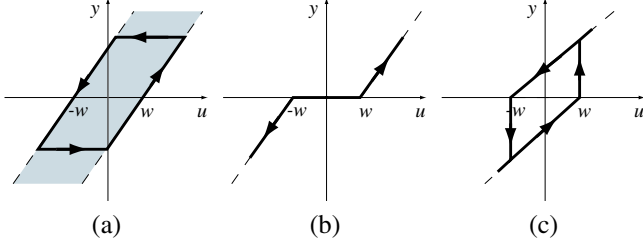
Fig. 10. The limiting periodic input-output map $\mathcal{H}_\infty(u)$ (solid) and the limiting equilibria set $\mathcal{E}$ (dashed) of (a) case 2, (b) case 3, and (c) case 4.

Case 2	$a_0 = 0$	hysteretic
Case 3	$a_0 \neq 0$ and $a_0 c_0 \geq 0$, or $a_0 \neq 0$ and $c_0(a_0 + c_0) < 0$	not hysteretic
Case 4	$a_0 \neq 0$ and $c_0(a_0 + c_0) > 0$	hysteretic if $\max_{t>0} u(t) \geq w$ and $\min_{t>0} u(t) \leq -w$.

TABLE I

CHARACTERISTICS OF $\mathcal{H}_\infty(u)$ OF THE DEADZONE-BASED BACKLASH HYSTERESIS MODEL WITH DIFFERENT CASES.

Then $\mathcal{E}$ is given by either (8), (9), or (10). Note that $\mathcal{E}$ cannot be given by (7) since, if $a_0 + c_0 = 0$, the equilibrium does not exist for constant inputs u such that $|u| > w$ and thus the system is not step convergent. Suppose $a_0 = 0$ (case 2) and thus $\mathcal{E}$ is given by (8). Then $\mathcal{E}$ is a multivalued map as shown in Figure 6b. Therefore $\mathcal{H}_\infty(u)$ is hysteretic as shown in Figure 10a. Now, suppose $a_0 \neq 0$ and $a_0 c_0 \geq 0$, or $a_0 \neq 0$ and $c_0(a_0 + c_0) < 0$ (case 3) and thus $\mathcal{E}$ is given by (9). Then $\mathcal{E}$ is a single-valued map as shown in Figure 6c. Therefore $\mathcal{H}_\infty(u)$ is not hysteretic as shown in Figure 10b. Finally, suppose $a_0 \neq 0$ and $c_0(a_0 + c_0) > 0$ (case 4) and thus $\mathcal{E}$ is given by (10). Then $\mathcal{E}$ is a single-valued map for $|u| < w$ and a multivalued map for $|u| > w$ shown in Figure 6d. Therefore $\mathcal{H}_\infty(u)$ is hysteretic when $\max_{t\geq 0} u(t) \geq w$ and $\min_{t\geq 0} u(t) \leq -w$ as shown in Figure 10c.

Table I summarizes the characteristics of $\mathcal{H}_\infty(u)$ for these cases.

Example 4.1: Consider (1), (2) with

$$A = \begin{bmatrix} 0 & 1 \\ -1 & -2 \end{bmatrix}, \quad B = \begin{bmatrix} 0 \\ 1 \end{bmatrix}, \quad C = \begin{bmatrix} 1 & 2 \end{bmatrix},$$

and $w = 0.5$. Since $a_0 = 1 \neq 0$ and $a_0 c_0 = 1 \geq 0$, the model satisfies case 3, and $\mathcal{H}_\infty(u)$ is not hysteretic from Table I. Figure 11 shows that the periodic input-output map converges to a single-valued map.

Example 4.2: Reconsider (1), (2) with

$$A = \begin{bmatrix} 0 & 1 \\ 1 & -2 \end{bmatrix}, \quad B = \begin{bmatrix} 0 \\ 1 \end{bmatrix}, \quad C = \begin{bmatrix} 2 & 0 \end{bmatrix},$$

and $w = 0.5$. Since $a_0 = -1 \neq 0$ and $c_0(a_0 + c_0) = 2 > 0$, the model is case 4, and $\mathcal{H}_\infty(u)$ is hysteretic from Table I. Figure 12 shows that the periodic input-output map converges to a hysteresis map.
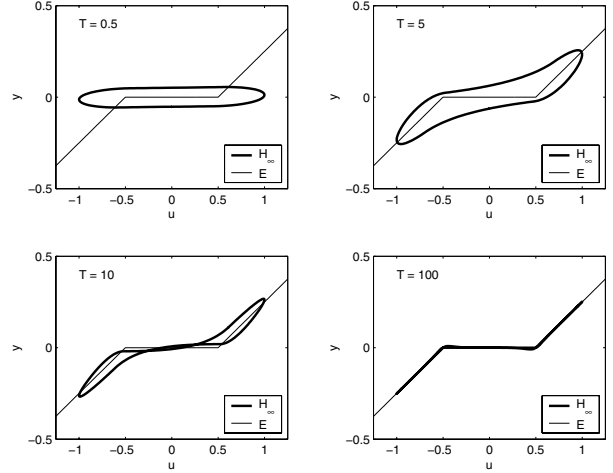

Fig. 11. $\mathcal{H}_T(u_T, y_T)$ and $\mathcal{E}$ for Example 4.1 with $u_T(t) = \sin\frac{2\pi}{T}t$. Note that this model is case 3 and is not hysteretic.
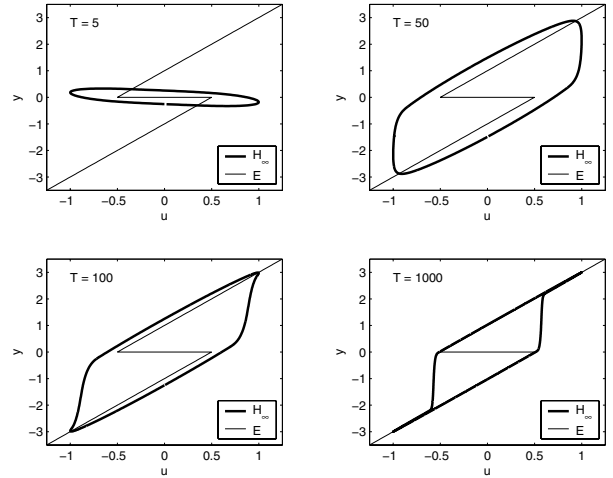

Fig. 12. $\mathcal{H}_T(u_T, y_T)$ and $\mathcal{E}$ for Example 4.2 with $u_T(t) = \sin\frac{2\pi}{T}t$. Note that this model is case 4 and $\mathcal{H}_T$ converges to a hysteresis map.

V. NONLINEAR FEEDBACK MODEL

As a generalization of the deadzone-based hysteresis model, consider the *nonlinear feedback model*

$$\dot{x}(t) = Ax(t) + D_1 u(t) + By_\phi(t), \tag{13}$$

$$y(t) = Cx(t) + D_2 u(t) + Dy_\phi(t), \tag{14}$$

$$u_\phi(t) = E_1 x(t) + E_0 u(t) + E_2 y_\phi(t), \tag{15}$$

$$y_\phi(t) = \phi\big(u_\phi(t)\big), \quad x(0) = x_0, \; t \geq 0, \tag{16}$$

where $\phi : \mathbb{R} \to \mathbb{R}$ is a memoryless nonlinearity. We assume that ϕ is globally Lipschitz and thus the solution of (13)–(16) exists and is unique on all finite intervals. Under these assumptions, x and y are C^1. We also assume that (A, B, C) is minimal.

Let $G_{11}(s) \triangleq C(sI_n - A)^{-1}D_1 + D_2$, $G_{12}(s) \triangleq C(sI_n - A)^{-1}B + D$, $G_{21}(s) \triangleq E_1(sI_n - A)^{-1}D_1 + E_0$, and $G_{22}(s) \triangleq E_1(sI_n - A)^{-1}B + E_2$. Then (13)–(16) can be interpreted as the linear fractional transformation
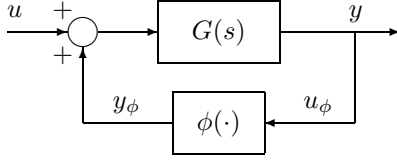
Fig. 13. Feedback interconnection of the nonlinear feedback model (17), (18), where $G(s) = C(sI - A^{-1})B$

between the nonlinearity $\phi(\cdot)$ and the transfer functions G_{11}, G_{12}, G_{21}, and G_{22}, which corresponds to the feedback interconnection of Figure 5.

The nonlinear feedback hysteresis model (13)–(16) can be simplified as follows. Let $E_2 = D = D_2 = E_0 = 0$, $D_1 = B$, and $E_1 = C$. Then (13)–(16) can be simplified as

$$\dot{x}(t) = Ax(t) + B\big(u(t) + \phi(y(t))\big), \qquad (17)$$

$$y(t) = Cx(t), \qquad x(0) = x_0, \quad t \geq 0. \qquad (18)$$

Figure 13 shows the feedback interconnection of (17), (18). Note that Figure 13 is a special case of Figure 5 with

$$\begin{bmatrix} G_{11}(s) & G_{12}(s) \\ G_{21}(s) & G_{22}(s) \end{bmatrix} = \begin{bmatrix} G(s) & G(s) \\ G(s) & G(s) \end{bmatrix}. \qquad (19)$$

Now, consider (13)–(16) with $E_2 = D = D_2 = 0$, $D_1 = 0$, $E_0 = 1$, and $E_1 = -C$. Then an alternative specialization of (13)–(16) is given by the deadzone-based hysteresis model (1), (2). Note that the feedback interconnection in Figure 2 is a special case of Figure 5 with

$$\begin{bmatrix} G_{11}(s) & G_{12}(s) \\ G_{21}(s) & G_{22}(s) \end{bmatrix} = \begin{bmatrix} 0 & G(s) \\ 1 & -G(s) \end{bmatrix}, \qquad (20)$$

and with $\phi = d_{2w}$.

The nonlinear feedback model can exhibit hysteresis maps of various shapes, see Figure 14. Each combination of linear dynamics and nonlinearities generates multiple attracting equilibria and multivalued limiting equilibria sets, and the step convergence of the closed-loop system gives rise to the hysteresis maps.

VI. Conclusion

In this paper we considered a nonlinear feedback model for hysteresis with emphasis on the deadzone nonlinearity. The relationship between step convergence and the hysteresis maps of the model was investigated. The class of models that exhibit hysteresis was determined and the shape of the hysteresis maps was related to the limiting equilibria set. The numerical examples verified the proposed analysis.

References

[1] D. N. Maywar, G. P. Agrawal, and Y. Nakano, "All-optical hysteresis control by means of cross-phase modulation in semiconductor optical amplifiers," *J. Opt. Soc. Amer. B*, vol. 18, no. 7, pp. 1003–1013, 2001.

[2] G. Cao and P. P. Banerjee, "Theory of hysteresis and bistability during transmission through a linear nondispersive-nonlinear dispersive interface," *J. Opt. Soc. Amer. B*, vol. 6, no. 2, pp. 191–198, 1989.
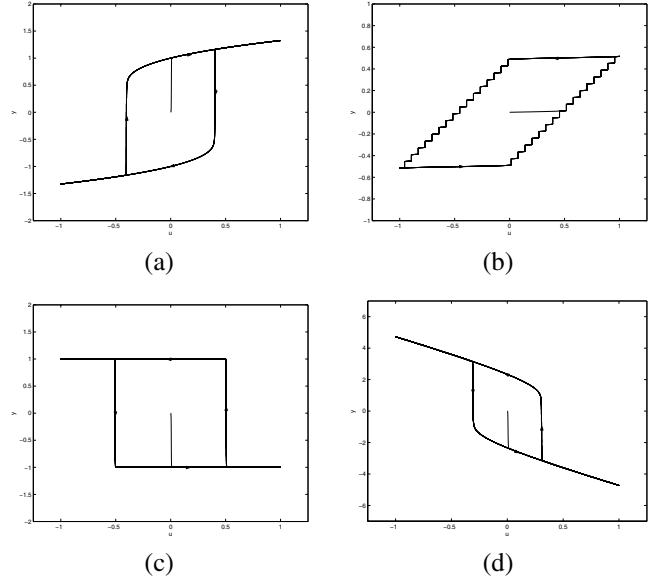
Fig. 14. The hysteresis maps for the nonlinear feedback model with various linear dynamics and nonlinearities. The model in Figure 13 with (a) $G(s) = \frac{1}{s-1}$ and $\phi(v) = -v^3$, (b) $G(s) = \frac{1}{s+1}$ and $\phi(v) = \frac{w}{2}\sin\eta v$ with $w = 1$ and $\eta = 1000$. The model in Figure 2 with (c) $G(s) = \frac{2}{s+1}$ and $d_{2w} = \tan^{-1}$, and (d) $G(s) = -\frac{2}{s+1}$ and $d_{2w} = \text{sat}_{0.5}$.

[3] N. F. Mitchell, J. O'Gorman, J. Hegarty, and J. C. Connoly, "Optical bistability and X-shaped hysteresis in laser diode amplifiers," in *Lasers and Electro-Optics Society Annual Meeting*, 1993, pp. 520–521.

[4] D. Angeli and E. D. Sontag, "Multi-stability in monotone input/output systems," *Sys. Contr. Lett.*, vol. 51, pp. 185–202, 2004.

[5] I. D. Mayergoyz, *Mathematical Models of Hysteresis*. New York: Springer-Verlag, 1991.

[6] L. O. Chua and S. C. Bass, "A generalized hysteresis model," *IEEE Trans. Circuit Theory*, vol. 19, no. 1, pp. 36–48, 1972.

[7] J. Oh and D. S. Bernstein, "Semilinear Duhem model for rate-independent and rate-dependent hysteresis," *IEEE Trans. Autom. Contr.*, 2005, to appear.

[8] A. Visintin, *Differential Models of Hysteresis*. New York: Springer-Verlag, 1994.

[9] M. Nordin and P. Gutman, "Controlling mechanical systems with backlash - a survey," *Automatica*, vol. 38, no. 10, pp. 1633–1649, 2002.

[10] M. Nordin, J. Galic, and P. Gutman, "New models for backlash and gear play," *Int. J. Adaptive Control and Signal Processing*, vol. 11, pp. 49–63, 1997.

[11] G. Tao and P. V. Kokotović, *Adaptive Control of Systems with Actuator and Sensor Nonlinearities*. New York: Wiley, 1996.

[12] C. Su, Y. Stepanenko, J. Svoboda, and T. P. Leung, "Robust adaptive control of a class of nonlinear systems with unknown backlash-like hysteresis," *IEEE Trans. Autom. Contr.*, vol. 45, no. 12, pp. 2427–2432, 2000.

[13] S. L. Lacy, D. S. Bernstein, and S. P. Bhat, "Hysteretic systems and step-convergent semistability," in *Proc. Amer. Contr. Conf.*, Chicago, IL, June 2000, pp. 4139–4143.

[14] D. S. Bernstein and S. P. Bhat, "Lyapunov stability, semistability, and asymptotic stability of matrix second-order systems," *ASME Trans. J. Vibr. Acoustics*, vol. 117, pp. 145–153, 1995.

[15] S. P. Bhat and D. S. Bernstein, "Nontangency-based Lyapunov tests for convergence and stability in systems having a continuum of equilibria," *SIAM J. Contr. Optimiz.*, vol. 42, pp. 1745–1775, 2003.

[16] C. D. Aliprantis and K. C. Border, *Infinite Dimensional Analysis: A Hitchhiker's Guide*, 2nd ed. Berlin: Springer-Verlag, 1999.